

NATIONAL ADVISORY COMMITTEE FOR AERONAUTICS

TECHNICAL NOTE 3309

MECHANICAL PROPERTIES AT ROOM TEMPERATURE OF
FOUR CERMETS OF TUNGSTEN CARBIDE
WITH COBALT BINDER

By Aldie E. Johnson, Jr.

Langley Aeronautical Laboratory
Langley Field, Va.



Washington

December 1954

TECHNICAL NOTE 3309

MECHANICAL PROPERTIES AT ROOM TEMPERATURE OF
FOUR CERMETS OF TUNGSTEN CARBIDE
WITH COBALT BINDER

By Aldie E. Johnson, Jr.

SUMMARY

Room-temperature stress-strain curves are presented for compression, tension, and shear loadings on four compositions of tungsten carbide with cobalt binder. Values of modulus of elasticity, modulus of rigidity, Poisson's ratio in the elastic region, ultimate strength, density, and hardness for the four materials are tabulated.

INTRODUCTION

The wider utilization of carbide-type cermets in applications at room temperature where the high values of modulus of elasticity and ratio of modulus to density could be used to advantage has been delayed because of insufficient knowledge of the mechanical properties of the various materials, particularly the shear and tensile properties. The available data on the properties of cermets are limited and are principally related to specific high-temperature applications. The present investigation of the properties of some cermets having a tungsten-carbide base is an extension of the investigation of the cermets having a titanium-carbide base reported in reference 1. Properties of four cermets having a tungsten-carbide base for compression, tension, and torsional shear loadings are given in the present paper. Complete stress-strain curves to failure were obtained in addition to values of modulus of elasticity, modulus of rigidity, Poisson's ratio, ultimate strength, hardness, and density. The materials tested were the following combinations of tungsten carbide with cobalt as a binder element:

WC, percent	Co, percent
97	3
94	6
90	10
85	15

The test specimens were fabricated by the hot-pressing technique at Kennametal, Inc.

DESCRIPTION OF SPECIMENS AND TESTS

The sizes and shapes of the specimens are shown in figure 1; specimens 1, 2, and 3 are compression, tension, and shear specimens, respectively. Two specimens of each of the four compositions were tested in each of the three loadings. The specifications for the surface finish of the specimens called for smooth grind and, in the case of the tensile specimens, an additional requirement of no transverse scratches visible with the naked eye and no longitudinal scratches exceeding 4 microinches in depth.

Inasmuch as the carbides are very hard and brittle, the experimental work of determining the mechanical properties, particularly the compressive strength, proved to be unusually difficult. Each of the three test-specimen shapes used in this investigation was designed especially for the material tested. The diameter and length of the test section of the tensile specimen corresponded to the proportions of standard round tensile specimens. The designs necessitated special grips and fixtures for the tension and torsion tests. The test specimens and testing techniques were the same as those described in reference 1; hence, they will be described only briefly in subsequent sections.

The volumes and weights of the compression specimens were used to determine the densities of the various compositions, and these are shown in table I. The hardness of the materials (also given in table I) was determined from superficial hardness tests (Rockwell 30-N scale).

Compression Tests

The compression test specimen shown in figure 1 is a column 3 inches long and 1 inch square, with end surfaces ground flat, parallel, and perpendicular to the specimen axis. For each specimen, the elastic longitudinal strains and elastic transverse strains were measured, and a load-strain curve was obtained to failure of the specimen. The elastic transverse strains were measured on two opposite faces of the specimen at several load increments with Tuckerman optical strain gages. Coincidentally with these measurements, the longitudinal strains on the remaining two faces of the specimen were measured with Baldwin SR-4 resistance wire strain gages (type AX-5). After the transverse strains had been determined, the load was removed from the specimen, and the transverse gages were replaced by Tuckerman optical gages in the longitudinal direction. The elastic longitudinal strains were determined similarly to the elastic transverse strains, and the wire strain gages on the remaining two faces were again used as a check on the consistency of loading between runs and also as a means to provide a continuous load-strain curve of the material to failure of the specimen. The longitudinal optical gages were

removed from the specimen at a load corresponding to about 25 percent of the ultimate load on the specimen, and the two wire strain gages were used to obtain the remainder of the load-strain curve. The stress-strain curve of the material was determined from the load-strain data, and Poisson's ratio was determined from the elastic values of longitudinal and transverse strains measured with the optical gages.

Tension Tests

The tension test specimen (specimen 2, fig. 1) had a test section $1/2$ inch in diameter by $2\frac{1}{4}$ inches long and a 1-inch-radius fillet which joined the test section to the 40° (included angle) conical ends. Load-strain curves were obtained from four wire strain gages (A-5) spaced equally around the circumference of the test section.

Shear Tests

The shear test specimens (specimen 3, fig. 1) were hollow cylinders of $1/8$ -inch wall thickness and $1\frac{1}{4}$ -inch outside diameter. The 2-inch-long test section was joined to the hexagonal ends by a fillet of $5/8$ -inch radius. Torque-strain records were obtained to failure of the specimens. Two wire-strain-gage rosettes (AR-1) on the outer surface of the test section were used to determine the strains.

RESULTS AND DISCUSSION

Stress-Strain Curves

Complete stress-strain curves (figs. 2 to 4) were obtained to the ultimate strength of each specimen. For the compression tests (fig. 2), the stress was determined as the load in the specimen P, divided by the original cross-sectional area of the specimen A, and the strains were obtained from both optical gages and wire strain gages. The compositions containing 90 percent tungsten carbide and 85 percent tungsten carbide exhibited sufficient ductility so that a yield stress σ_{cy} (0.2-percent offset) could be determined.

For the tension tests (fig. 3), the stress was determined as the P/A stress, and the strain was obtained as the average strain of the four wire gages. In all cases, failure occurred before a yield stress corresponding to 0.2-percent offset was reached. For the composition which had the greatest strain (85 percent tungsten carbide), a strain of only 0.0015 was achieved before failure.

For the torsion test, the outer-surface shear strain γ_o was computed from the outer-surface compressive and tensile strains measured by the elements of the wire-strain-gage rosette at angles of 45° on either side of the longitudinal axis of the specimen. With the compressive direction taken as positive, the equation is

$$\gamma_o = \epsilon_1 - \epsilon_2$$

where

ϵ_1 compressive strain

ϵ_2 tensile strain

Thus, a torque—shear-strain curve was determined from the original torque-strain curves.

An expression for the outer-surface shear stress in a twisted hollow cylinder can be derived in a manner similar to that given in reference 2 for the case of a solid cylinder. The resulting equation is

$$\tau_o = \frac{1}{2\pi r_o^3} \left(\gamma_o \frac{dT}{d\gamma_o} + 3T \right) + \tau_i \left(\frac{r_i}{r_o} \right)^3$$

where

τ_o, τ_i shear stress at outer and inner surfaces, respectively

T applied torque

r_o, r_i outer and inner radii, respectively, of the cylindrical test section

The shear stress-strain curves were determined from this torque—shear-stress relation and the torque—shear-strain curves. In the elastic-stress range, the torque-stress equation reduces to the familiar form

$$\tau_o = \frac{2T}{\pi r_o^3 \left[1 - \left(\frac{r_i}{r_o} \right)^4 \right]}$$

which may also be used in the inelastic-stress range to determine an approximate relationship between applied torque and outer-surface shear

stress. The approximate stress-strain curve determined from the elastic-stress-torque equation was then used in conjunction with the general torque-stress equation to calculate an improved stress-strain curve. For given values of torque, values of τ_i were read from the approximate stress-strain curve at values of strain compatible with the assumption that the shear strain varies linearly from the longitudinal axis of the cylinder to the outer surface, and values of τ_o were then determined from the general equation. Successively improved stress-strain curves were computed until convergence was obtained. The final shear stress-strain curves for the torsion specimens are given in figure 4.

Elastic Properties

The elastic properties of the four materials determined from the stress-strain curves are modulus of elasticity E from the compressive and tensile curves and modulus of rigidity G from the shear curves. In addition, Poisson's ratio μ was determined for the compression specimens. The elastic properties are given in table I, and their variations with the composition of the material are shown in figure 5. Because the tensile and compressive values of modulus of elasticity are similar and the compressive values were determined with a higher degree of accuracy, the tensile test points have been omitted from figure 5.

The modulus of elasticity and modulus of rigidity are highest for a material composed of 97 percent tungsten carbide and 3 percent cobalt, and both moduli decrease with increasing amounts of binder. Poisson's ratio appears to increase slightly with increasing amounts of binder material.

Values of the ratio of modulus to density for the four compositions tested are given in table I. Although the elastic moduli for the cermets having a tungsten-carbide base are extremely high, the ratios of modulus to density are only about one-half the values for the cermets having a titanium-carbide base reported in reference 1. The values for cermets having a tungsten-carbide base, however, are appreciably higher than those for the common structural materials which are in the range 90,000 to 110,000 ksi/lb/cu in.

As a check on the values of G determined from the shear stress-strain curve, the values of E and μ determined from the compression tests of each material were substituted into the equation for an isotropic material,

$$G = \frac{E}{2(1 + \mu)}$$

and values of G (called G_{calc} in table I) were computed. These values are in good agreement with the values of G determined from the torsion tests.

Strength

The compressive and tensile strengths were determined as the highest value of P/A stress in each test. The shear strengths were computed from the maximum moment and maximum shear strain as described in a previous section. These test data are given in table I.

In figure 6(a), curves have been faired through the present test data to show the variation in ultimate strength for the three loadings in terms of the composition of the material. The ultimate tensile and compressive strengths appear to be highest for the material having about 10 percent cobalt binder material; whereas the ultimate shear strength appears to increase slightly with increasing amounts of binder material.

A comparison of the ultimate compressive strengths of the present tests and other tests of tungsten carbide with cobalt binder reported in references 3 and 4 is given in figure 6(b). The results of the present tests are considerably lower than the previously reported data. Two possible explanations for this discrepancy are differences in specimen size and shape and in test technique between the present and previously reported tests. The previous tests were run on columns 3/4 inch long and 1/2 inch square with thin brass buffer plates between the specimen ends and the hardened bearing blocks. In order to determine whether or not the difference in strength could be attributed to the use of buffer plates, two additional specimens (3 inches long and 1 inch square) of a composition having 94 percent tungsten carbide and 6 percent cobalt were tested by using buffer plates of brass shim stock 0.020 inch thick. These tests (see table I) showed no increase in strength over specimens of the same size and shape tested without buffer plates. Thus, the difference in specimen size and shape appears to be the primary reason for the differences in compressive strength between the present tests and those reported in references 3 and 4. Because the longer length of the present specimens tends to reduce the effect of the restriction on Poisson's expansion occurring at the ends of the specimen and hence provides a larger amount of material subject to a uniaxial stress condition, the results of the present tests on the longer specimens are believed to be more nearly representative of the uniaxial compressive strength of the material.

The failures of the compression and tension specimens were failures typical of brittle materials. The failure of the shear specimens was similar to those reported in reference 1 and indicated that the failure occurred along planes inclined approximately 45° to the longitudinal axis of the specimens.

CONCLUDING REMARKS

Room-temperature stress-strain curves are presented for compression, tension, and shear loadings on four different compositions of tungsten carbide with cobalt binder. Values of modulus of elasticity, modulus of rigidity, Poisson's ratio in the elastic region, ultimate strength, density, and hardness for the four materials are tabulated. The very high values of compressive strength and modulus of elasticity, as well as the ratios of modulus to density, which are somewhat higher than those of the more common materials, indicate possible advantageous uses of the materials in special applications where the more common materials are not adequate. However, suitable design precautions should be exercised with regard to the wide variation in compressive ultimate strength, apparently associated with specimen size and shape, and also with regard to the lack of ductility and the relatively low and highly variable tensile and shear strengths of these cermets.

Langley Aeronautical Laboratory,
National Advisory Committee for Aeronautics,
Langley Field, Va., August 31, 1954.

REFERENCES

1. Johnson, Aldie E., Jr.: Mechanical Properties at Room Temperature of Four Cermets of Titanium Carbide With Nickel Binder. NACA TN 3197, 1954.
2. Nádai, A.: Theory of Flow and Fracture of Solids, Vol. I, second ed., McGraw-Hill Book Co., Inc., 1950, pp. 347-349.
3. Hull, L. J., and Schwartz, D. L.: Cemented or Sintered Carbides. Metals Handbook, Taylor Lyman, ed., A.S.M. (Cleveland, Ohio), 1948, p. 62. (Reprinted 1952.)
4. Anon.: Kennametal Cemented Carbide Products. Catalog 49, Kennametal Inc. (Latrobe, Pa.), May 1949.

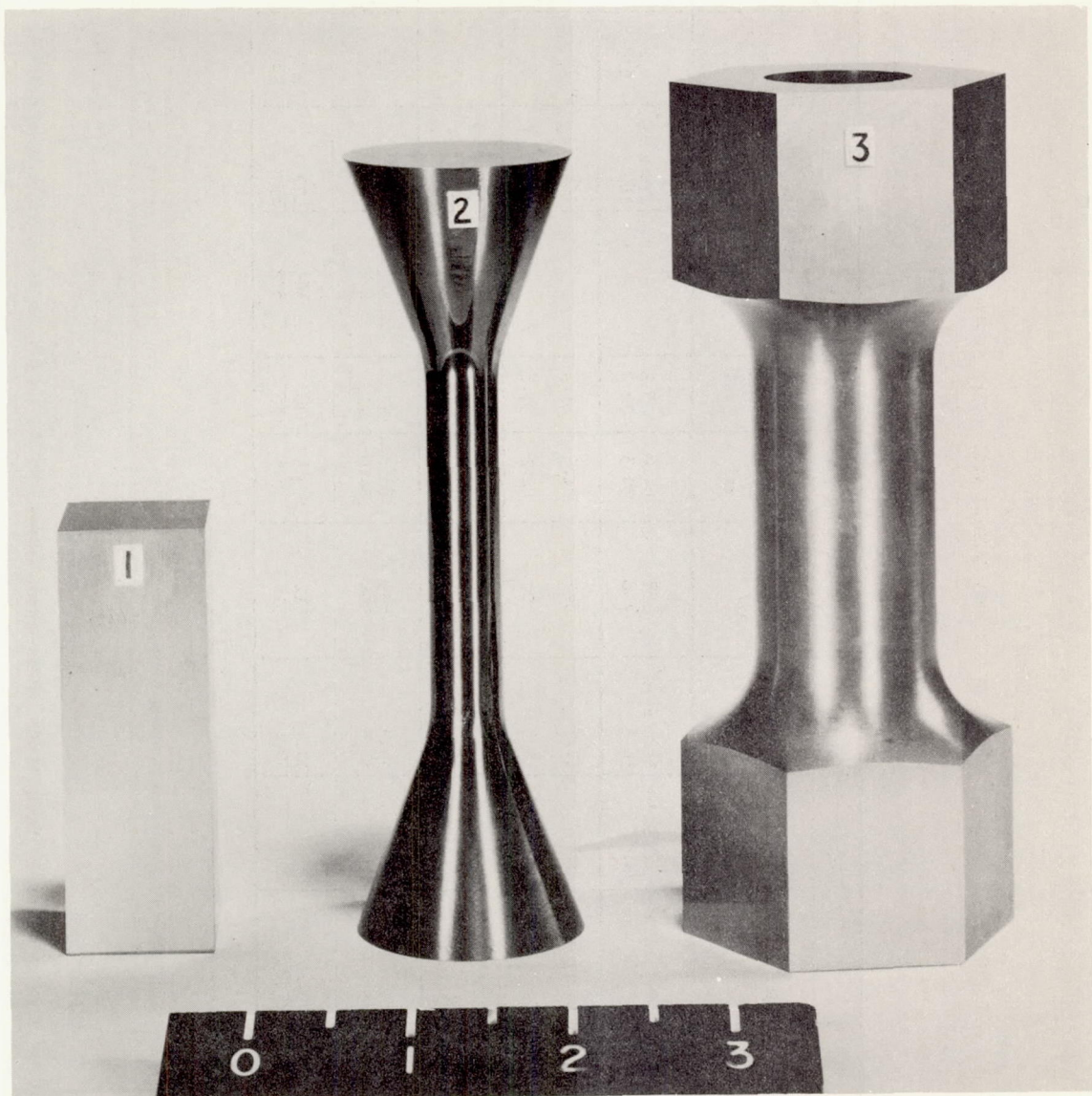
TABLE I
PROPERTIES OF CERMETS COMPOSED OF TUNGSTEN CARBIDE WITH COBALT BINDER

Compo- sition		Density, lb/cu in.	Hardness, Rockwell 30-N scale	Poisson's ratio, μ	Modulus in -			Ultimate strength in -			Compressive yield stress, σ_{cy} , ksi	Modulus Density, ksi lb/cu in.	Tension fracture (a)	Modulus in shear, G_{calc} , ksi
					Compression, E, ksi	Tension, E, ksi	Shear, G, ksi	Compression, σ_{max} , ksi	Tension, σ_{max} , ksi	Shear, τ_{max} , ksi				
WC, %	Co, %													
97	3	0.554	90	0.22 .21	94.4×10^3 93.2	94.4×10^3 93.8	38.6×10^3 38.3	488 458	64.8 59.3	93.2 72.8		170×10^3 169	1/2 5/8	38.6×10^3
94	6	.539	87	.22	91.3	95.4	37.7	542	81.6	61.9		169	^b $\frac{1}{4}$ $\frac{1}{8}$	37.5
				.21	90.8	90.4	36.5	526	82.1	97.8		169		
		c.527	--	----	c89.2 c88.0			c512 c533				169 167		
90	10	.525	85	.22 .22	83.6 83.5	84.4 81.8	35.5 34.5	555 556	88.8 154.4	145 121	466 474	159 159	1 1	34.2
85	15	.506	85	.23 .22	76.1 75.8	76.8 58.7	30.4 30.1	511 510	119.4 65.5	128 135	366 372	150 150	1/4 1	31.0

^aDistance from fracture to center of test section, in.

^bIn fillet.

^cTests run with 0.020-inch brass sheet between specimen and bearing blocks.



L-75396.1

Figure 1.—Compression, tension, and shear test specimens.

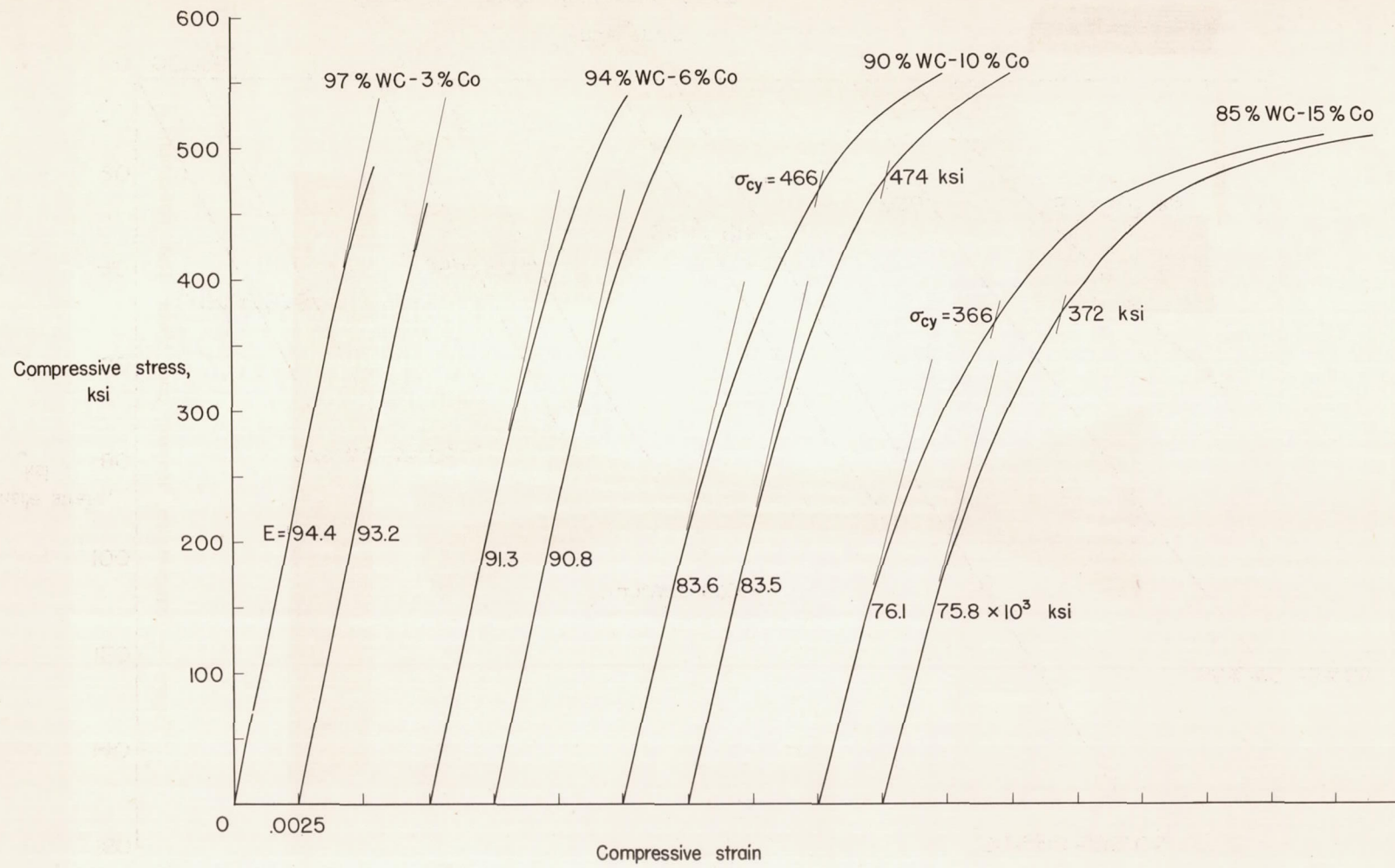


Figure 2.—Compressive stress-strain curves.

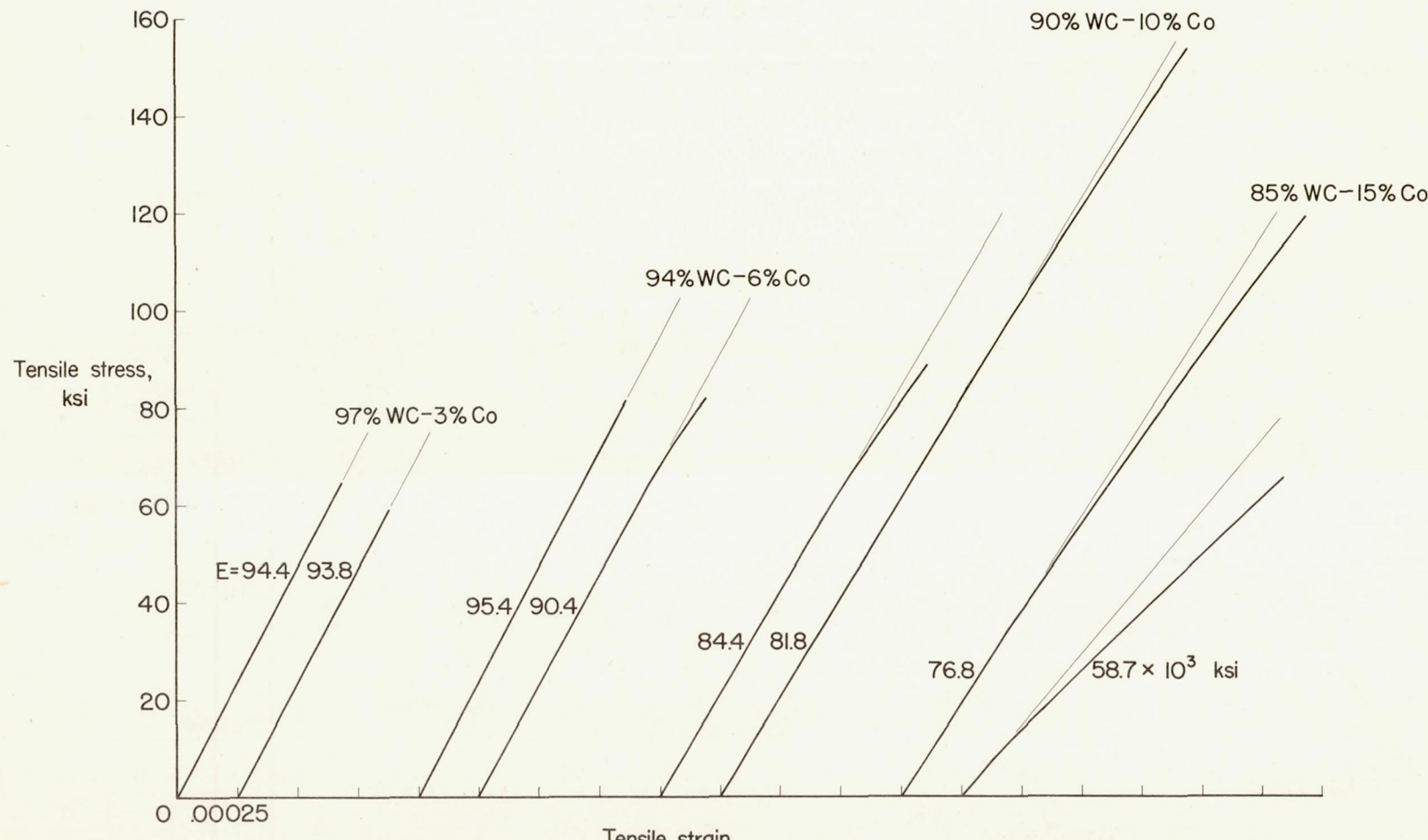


Figure 3.—Tensile stress-strain curves.

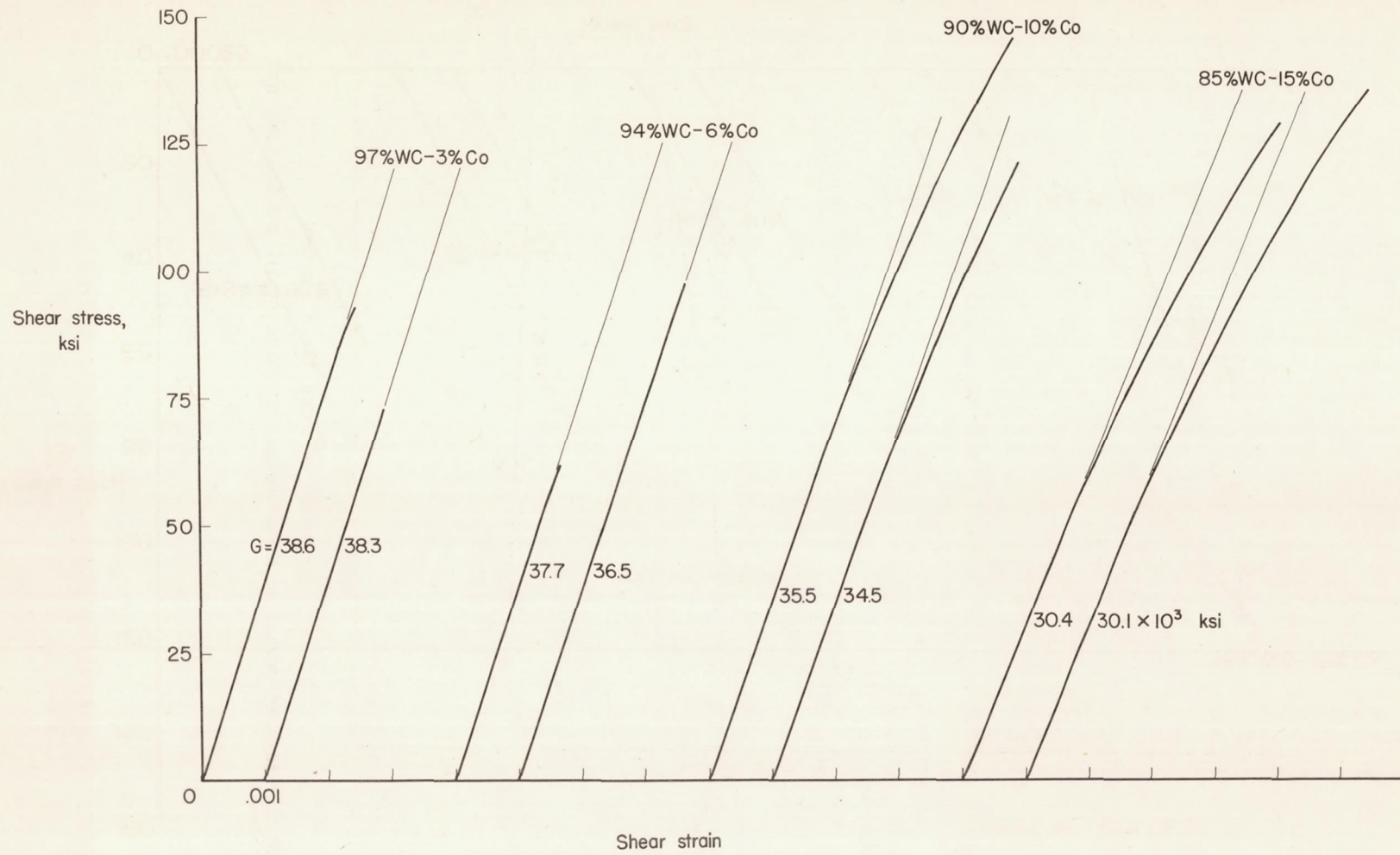


Figure 4.—Shear stress-strain curves.

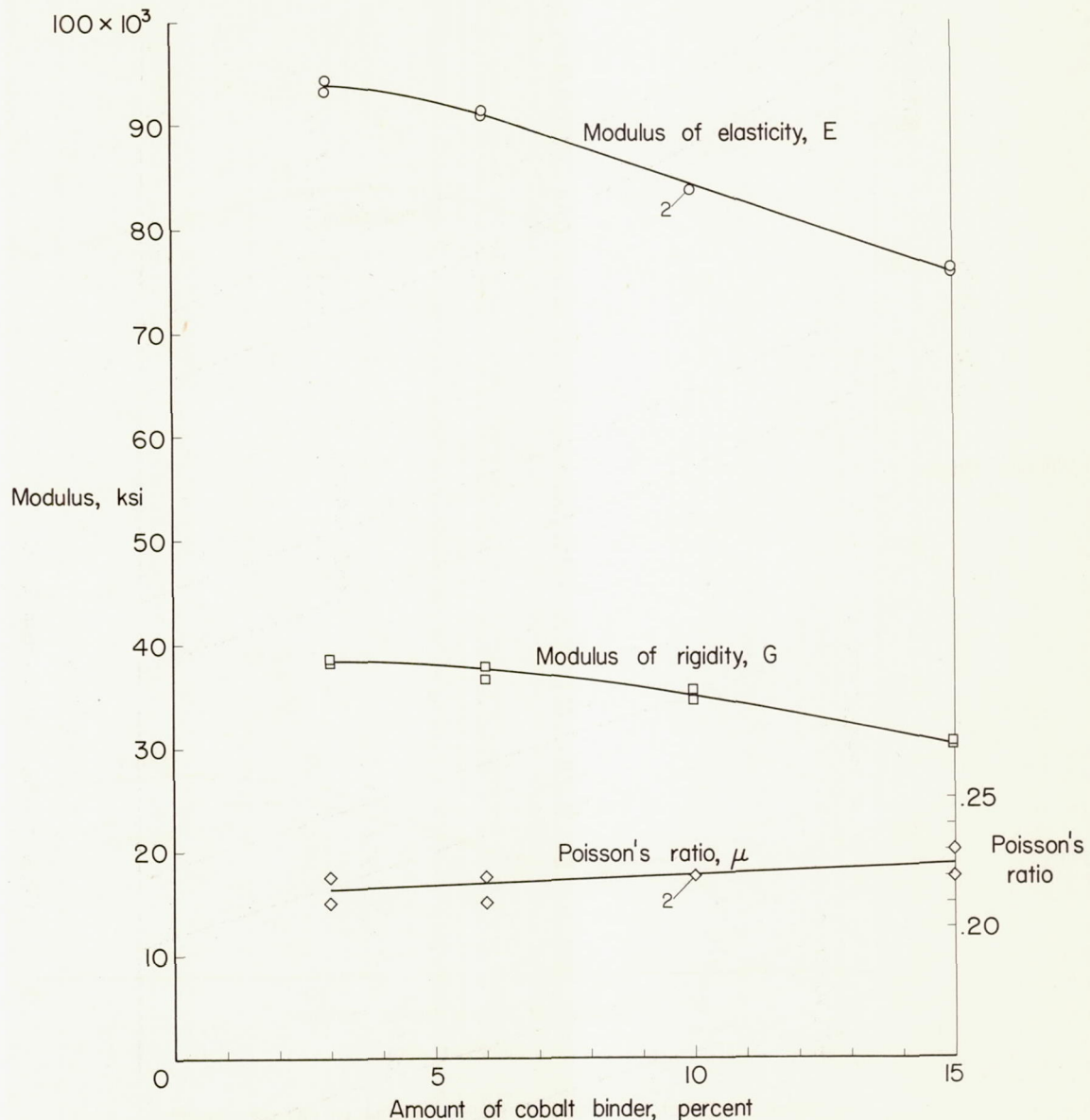


Figure 5.—Effect of amount of binder material on elastic moduli and Poisson's ratio.

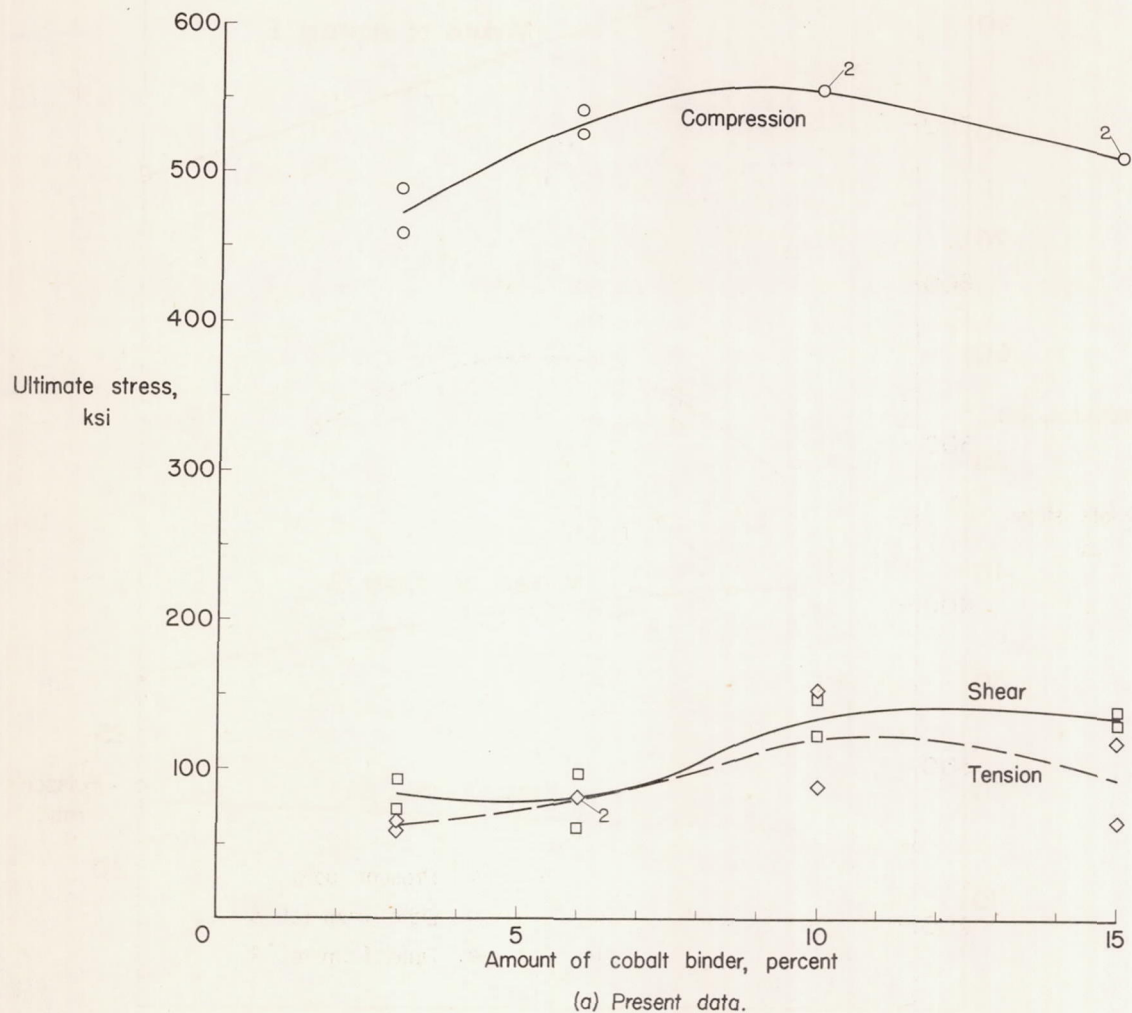
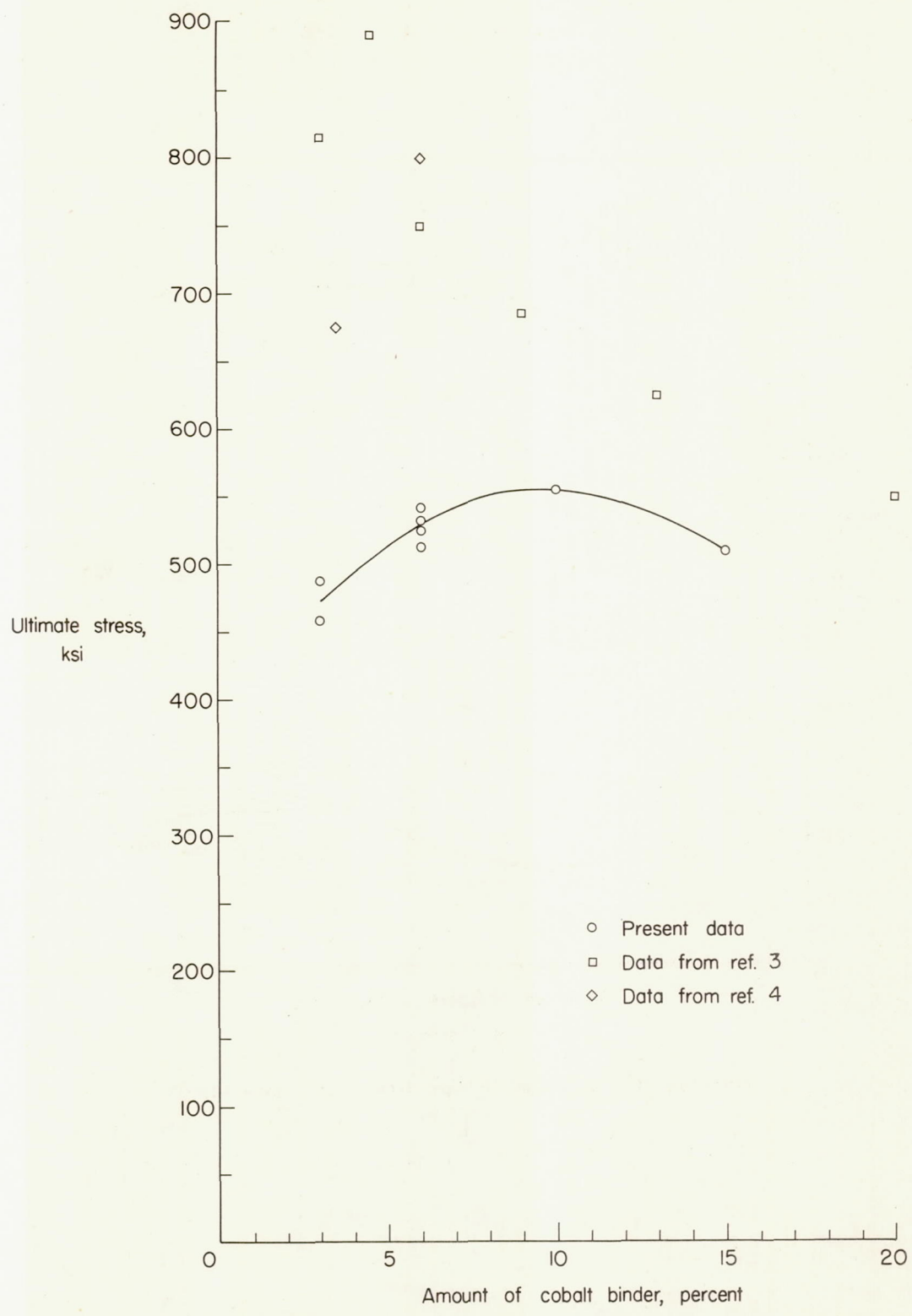


Figure 6.—Effect of amount of binder material on ultimate strength.



(b) Comparison with previous data for compressive strength.

Figure 6.-Concluded.